Shape Optimization of a Membrane Wing for Micro Air Vehicles

Yongsheng Lian,* Wei Shyy,† and Raphael T. Haftka‡
University of Florida, Gainesville, Florida 32611

Nomenclature

B	=	half-wing span
C	=	chord length
C_D	=	drag coefficient of a wing
C_L	=	lift coefficient of a wing
C_L/C_D	=	lift-to-drag ratio
c_d	=	drag coefficient of a cross-section airfoil
c_l	=	lift coefficient of a cross-section airfoil
x	=	chordwise distance from the leading edge
Y_i	=	design variable
z	=	spanwise distance from the root
α	=	angle of attack

Introduction

In recent years there has been growing interest in micro air vehicles.[1] One notable approach is to use a flexible membrane wing to improve aerodynamic performance.[1] Previous studies of membrane wings were largely based on empirical observations,[2] two-dimensional viscous-flow-based computations,[3] and simplified three-dimensional analyses.[4] Recently, Lian et al.[5] adopted a dynamic membrane model to examine the aerodynamic and structural characteristics of a three-dimensional membrane wing. In their study, full Navier–Stokes equations, a hyperelastic membrane model, a moving grid technique, and an interface scheme were integrated to facilitate such computations.

To gain a more systematic understanding of possible membrane wing performance, we conduct a gradient-based shape optimization and assess the characteristics of both rigid and membrane wings. The optimization of a membrane wing introduces two challenges. First, coupled, time-dependent simulations of interactions between viscous fluid flow and a flexible structure are very expensive. Second, efficient and automatic grid regeneration is essential for both the fluid/structure interaction and shape optimization. This Note deals with these issues by using the following strategies:

1) Instead of optimizing the membrane wing directly, we optimize a rigid wing as a surrogate and then check the membrane wing performance based on the outcome of the surrogate model. This may be considered as a first step in using the surrogate in more elaborate methods.[6–9] The optimizer Design Optimization Tools (DOT)[10] using sequential quadratic programming then perturbs one or more design variables.

2) We automate a moving grid technique by treating the optimization process as a "moving boundary problem."[3] This technique facilitates not only the optimization process but also the computation of fluid and membrane wing interactions. The detailed information is given in Lian et al.[11]

Optimization and Computational Approaches

The objective is to improve the lift-to-drag ratio of a membrane wing under constraints. The baseline membrane wing shape is chosen from a series of trial-and-error exercises with little direct insight from the three-dimensional aerodynamics of a low-aspect wing. Only the wing shape is considered in this work; neither the fuselage nor the propeller is included. The baseline wing has a variable spanwise camber: 7.5% at the root and 2% at the tip. The wing, based on a three-batten arrangement, has a maximal chord length of 13.7 cm, a mean chord of 9.4 cm, and a span of 15 cm. The angle of attack is defined in reference to the root geometry. The design point of the present MAV flies at a speed of 10 m/s and an angle of attack of 6 deg. Because there is no change in weight in the level flight under battery power, this optimization exercise is solved as a single-point problem.

The wing surface can be implicitly represented by a function $y = f(x, z)$, where x, y, and z represent the wing surface coordinates. We choose six design variables corresponding to six points on the wing surface. Three are located at the root at 10%, 27%, and 77% of the chord. The other three are located at batten 2 with the same relative chord positions. We use Y_i to designate a design variable, which is defined as the perturbation of a baseline value at point i. We interpolate perturbations from all of the design variables over the wing surface with the thin plate spline (TPS) interpolation,[12] which ensures that the interpolated surface has a second-order continuity:

$$\delta y(x, z) = G(\boldsymbol{Y}) \tag{1}$$

where $\boldsymbol{Y} = (Y_1, Y_2, \ldots, Y_6)$ is the design variable vector, G is the TPS interpolation operator, and δy is the interpolated value over the wing surface. The perturbed wing surface is then represented as $y^{\text{new}} = y + \delta y$. An advantage of this perturbation approach is that we can recover the original shape when the perturbation $\boldsymbol{Y}$ is zero. In our optimization we fix both leading and trailing edges to maintain

Table 1 Design variables bounds and their optimal values at 6 deg

Parameter	Initial design	Lower bound	Upper bound	Optimal value
X_1	0.00	−0.40	0.00	−0.258
X_2	0.00	−0.40	0.00	−0.400
X_3	0.00	−0.20	0.20	−0.152
X_4	0.00	−0.20	0.20	−0.100
X_5	0.00	−0.10	0.20	−0.082
X_6	0.00	−0.10	0.20	0.135
Number of analyses				97
Number of cycles				6
C_L	0.530	0.529		0.529
C_L/C_D	7.06			7.55

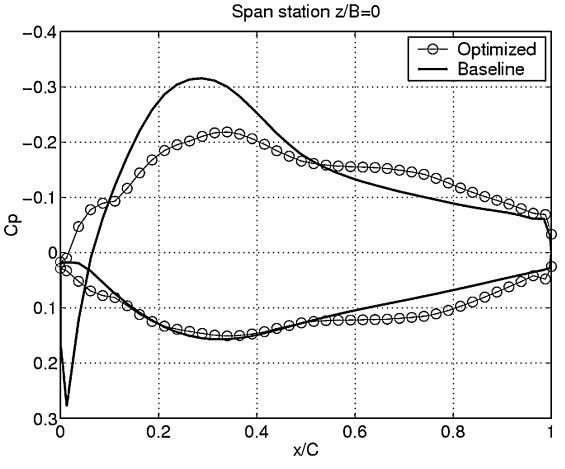

Fig. 1 Pressure coefficients at the root at an angle of attack of 6 deg.

Received 5 November 2002; presented as Paper 2003-0106 at the 41st Aerospace Sciences Meeting, Reno, NV, 6–9 January 2003; accepted for publication 8 July 2003.

*Ph.D. Student, Department of Mechanical and Aerospace Engineering; currently Senior Researcher, Ohio Aerospace Institute, Cleveland, OH 44142. Member AIAA.

†Professor and Chair, Department of Mechanical and Aerospace Engineering. Fellow AIAA.

‡Distinguished Professor, Department of Mechanical and Aerospace Engineering. Fellow AIAA.

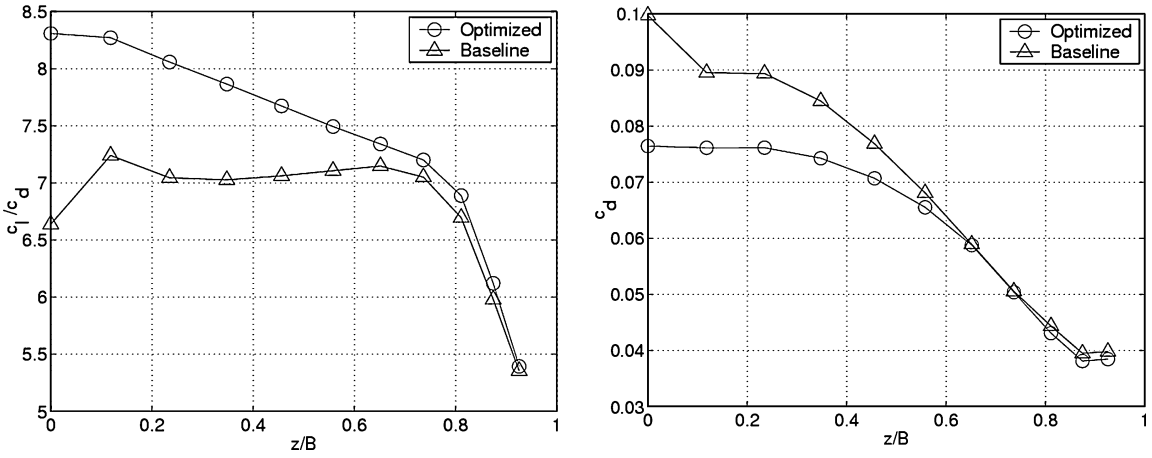

Fig. 2 Spanwise aerodynamic coefficient distributions at angle of attack of 6 deg.

the identical angle of attack between the baseline and optimized wings.

The present optimization problem can be formulated as follows:

$$\begin{aligned} &\text{Maximize} \qquad C_L/C_D \\ &\text{subject to} \\ &\quad 1)\ C_L \geq C_{L\,\text{baseline}} \\ &\quad 2)\ \text{Convexity constraint: } \frac{Y_1 + y_1 - y_0}{x_1 - x_0} \geq \frac{Y_2 + y_2}{x_2 - x_0} \\ &\quad 3)\ Y_i^L \leq Y_i \leq Y_i^U, \qquad i = 1, 6 \end{aligned} \tag{2}$$

Constraint 1 requires that the lift coefficient of the optimized wing be no less than that of the baseline wing. Constraint 2 maintains the convexity of the airfoil to eliminate obviously inappropriate shapes. Constraint 3 gives the lower and upper bounds of the design variables whose values are listed in Table 1.

The optimization procedure begins with the baseline design. After the perturbation, the TPS interpolation is used to generate the entire wing surface. Next a computational grid is generated with the moving grid technique for the perturbed shape, and the Navier–Stokes solver is used to evaluate the objective function. A design cycle includes the evaluation of derivatives of the objective function and constraints (here by finite differences) and a one-dimensional search in a direction selected based on the derivatives. The search terminates when the DOT convergence criteria are satisfied.

The automated moving grid technique allows the optimization to proceed as a series of artificial "moving boundary problems" in which the moving grid technique guides the grid generation without human intervention. For the membrane wing computation one has to consider the shape change under external forces. This, of course, results in a time-dependent moving boundary problem, which can be solved by the same moving grid technique, as detailed in Ref. 5.

Results and Discussion

Instead of optimizing the membrane wing directly, we optimize a rigid wing as a surrogate, decoupling the aerodynamics and structural analyses. On the basis of the optimization output we evaluate both rigid and membrane wing performance. The optimization results, summarized in Table 1, improve the lift-to-drag ratio from 7.06 to 7.55. By doing so, the camber reduces from 7.5% to 4.8% near the root and increases from 2% to 4% near the tip. Figure 1 compares the spanwise pressure distributions on both wings. At the root, the baseline wing yields a cross-over pressure distribution at the leading edge, which decreases the total lift force. The optimized shape eliminates the cross over and gives a smoother distribution.

The spanwise c_l/c_d distribution is depicted in Fig. 2. The aerodynamic improvement is largely realized in the inner 70% of the wingspan. By reducing the camber in the root region, the optimized shape reduces the drag coefficient noticeably there, which leads to a higher overall lift-to-drag ratio. The overall aerodynamics of the membrane wings, for both baseline and optimized shapes, is summarized in Fig. 3. The optimized shape improves C_L/C_D, with more substantial improvement at modest angles of attack.

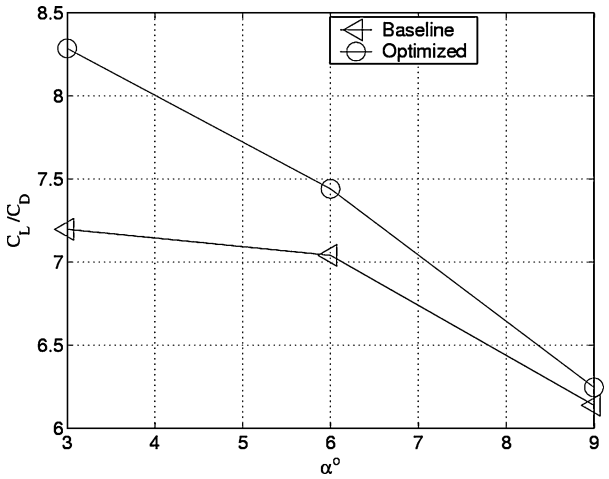

Fig. 3 Time-averaged membrane wing performance vs angles of attack.

Summary

We have performed an optimization of a flexible membrane wing using a rigid wing as surrogate. An analysis of the final design has verified that the flexible wing can be improved by optimization of a rigid wing with the same geometry. Compared to the baseline, the optimization leads to lower camber near the root and higher camber near the tip, while still leaving the camber slightly higher at the root than the tip. The lift-to-drag ratio improved over a range of angles of attack. However, at large angles of attack, the improvement with the optimized shape diminishes. At low angles of attack, the improvement is largely located within 70% of the inner wing. The improvement in aerodynamics of the optimized wing is largely realized via reduced-form drag and better pressure distributions.

Acknowledgments

The present work is supported by the Air Force Office of Scientific Research and the Industrial Technology Research Institute of Taiwan, Republic of China. The authors thank Satchi Venkataraman for helpful discussions.

References

[1]Shyy, W., Berg, M., and Ljungqvist, D., "Flapping and Flexible Wings for Biological and Micro Vehicles," *Process in Aerospace Sciences*, Vol. 35, 1999, pp. 455–506.

[2]Ifju, P., Jenkins, D., Ettinger, S., Lian, Y., Shyy, W., and Waszak, R. M., "Flexible-Wing-Based Micro Air Vehicles," AIAA Paper 2002-0705, Jan. 2002.

[3]Shyy, W., Udaykumar, H. S., Rao, M. M., and Smith, R. W., *Computational Fluid Dynamics with Moving Boundaries*, Taylor and Francis, Philadelphia, 1996, pp. 31, 32.

[4]Jackson, P. S., and Christie, G. W., "Numerical Analysis of Three-Dimensional Elastic Membrane Wings," *AIAA Journal*, Vol. 25, 1987, pp. 676–682.

[5]Lian, Y., Shyy, W., Ifju, P. G., and Verron, E., "Membrane Wing Model for Micro Air Vehicles," *AIAA Journal*, Vol. 41, No. 12, 2003, pp. 2492–2494.

[6]Hutchison, M. G., Unger, E. R., Mason, W. H., Grossman, B., and Haftka, R. T., "Variable-Complexity Aerodynamic Optimization of a High-Speed Civil Transport Wing," *Journal of Aircraft*, Vol. 31, 1994, pp. 110–116.

[7]Burgee, S., Giunta, A. A., Narducci, R., Watson, L. T., Grossman, B., and Haftka, R. T., "A Coarse Grained Parallel Variable-Complexity Multidisciplinary Optimization Paradigm," *International Journal of Supercomputer Applications and High Performance Computing*, Vol. 10, 1996, pp. 269–299.

[8]Mason, B. H., Haftka, R. T., Johnson, E. R., and Farley, G. L., "Variable Complexity Design of Composite Fuselage Frames by Response Surface Techniques," *Thin Wall Structures*, Vol. 32, 1998, pp. 235–261.

[9]Knill, D. L., Giunta, A. A., Baker, C. A., Grossman, B., Mason, W. H., Haftka, R. T., and Watson, L.T., "Response Surface Methods Combining Linear and Euler Aerodynamics for Supersonic Transport Design," *Journal of Aircraft*, Vol. 36, 1999, pp. 75–86.

[10]*Design Optimization Tools*, Vanderplaats Research and Development, Inc., Colorado Springs, CO, 1999.

[11]Lian, Y., Shyy, W., and Haftka, R. T., "Shape Optimization of a Membrane Wing for Micro Air Vehicles," AIAA Paper 2003-0106, Jan. 2003.

[12]Duchon, J. P., "Splines Minimizing Rotation-Invariant Semi-Norms in Sobolev Spaces," *Constructive Theory of Functions of Several Variables*, edited by W. Schempp and K. Zeller, Springer-Verlag, Berlin, 1977, pp. 85–100.

A. Plotkin
Associate Editor

Benchmark Solution of Laminated Beams with Bonding Imperfections

W. Q. Chen,* J. Ying,† J. B. Cai,‡ and G. R. Ye‡
Zhejiang University, 310027 Hangzhou, People's Republic of China

Introduction

THE effect of interlaminar bonding imperfections on responses of laminated/sandwich beams, plates, or shells has received much attention recently. Most of the available works have employed various simplified beam, plate, or shell theories in which certain assumptions on the elastic fields along the thickness direction are introduced.[1–5] More recently, we presented a three-dimensional study of cross-ply laminated rectangular plates with imperfect interfaces, based on the so-called state-space formulations.[6] Through comparison, it was shown that the accuracy of the extended zig-zag plate theory[1] would become worse with the increasing imperfections of interfaces. In addition, the prediction of interfacial imperfections of a practical structure from the plate theory, when compared to the experimental results of deflection, will result in an underestimated value. This is usually not favorable to the practical damaged structures. Thus, although there are many highly accurate simplified theories or numerical methods for perfect laminated/sandwich beams,[7–10] it seems necessary to develop exact solutions that can be used as benchmarks for the analysis of imperfect laminated/sandwich beams.

This Note presents an exact solution of simply supported cross-ply laminated beams featuring interlaminar bonding imperfections described by a spring-layer model.[1–4] The analysis is similar to that presented in our previous work,[6] but the state-space formulations are established based on the two-dimensional elasticity equations for the plane-stress problem. The state-space approach is very effective in analyzing laminated beams because the scale of the final solving equations is independent of the number of layers. The numerical results presented in this Note should provide a useful means of comparison in the development of simplified theories for imperfect laminated/sandwich beam structures.

State-Space Approach for Plane-Stress Problem

An N-layered cross-ply laminated beam is shown in Fig. 1. The three-dimensional constitutive relations for a cross-ply laminate can be found in Ref. 6, for example. For a beam structure, because the width is very thin and the load along the width stays invariant, the problem can be regarded as a plane-stress problem.[11] In this case, the nonzero stress components are σ_x, σ_z, and τ_{xz} only, which are independent of y. Then we can derive the following two-dimensional constitutive relations:

$$\sigma_x = C_{11}\frac{\partial u}{\partial x} + C_{13}\frac{\partial w}{\partial z}, \qquad \sigma_z = C_{13}\frac{\partial u}{\partial x} + C_{33}\frac{\partial w}{\partial z}$$

$$\tau_{xz} = C_{55}\left(\frac{\partial u}{\partial z} + \frac{\partial w}{\partial x}\right) \tag{1}$$

where u and w are the displacements in the x and z directions, respectively, and C_{ij} are the reduced stiffness constants, which can be expressed by the elastic constants c_{ij} as

$$C_{11} = c_{11} - c_{12}^2/c_{22}, \qquad C_{13} = c_{13} - c_{12}c_{23}/c_{22}$$

$$C_{33} = c_{33} - c_{23}^2/c_{22}, \qquad C_{55} = c_{55} \tag{2}$$

From Eq. (1) and the equations of motion,[11] the following state equation[12] can be obtained:

$$\frac{\partial}{\partial z}\begin{Bmatrix}\sigma_z\\ u\\ w\\ \tau_{xz}\end{Bmatrix} = \begin{bmatrix} 0 & 0 & \rho\dfrac{\partial^2}{\partial t^2} & -\dfrac{\partial}{\partial x}\\ 0 & 0 & -\dfrac{\partial}{\partial x} & \dfrac{1}{C_{55}}\\ \dfrac{1}{C_{33}} & -\dfrac{C_{13}}{C_{33}}\dfrac{\partial}{\partial x} & 0 & 0\\ -\dfrac{C_{13}}{C_{33}}\dfrac{\partial}{\partial x} & \rho\dfrac{\partial^2}{\partial t^2} - \alpha\dfrac{\partial^2}{\partial x^2} & 0 & 0 \end{bmatrix}\begin{Bmatrix}\sigma_z\\ u\\ w\\ \tau_{xz}\end{Bmatrix} \tag{3}$$

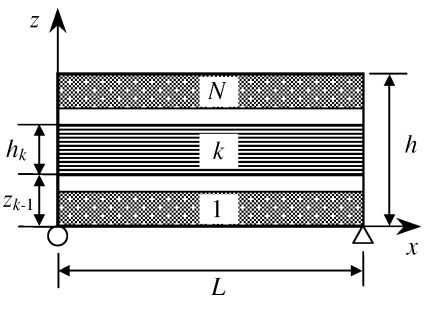

Fig. 1 Geometry and coordinates of a laminated beam.

Received 23 August 2003; revision received 13 September 2003; accepted for publication 15 September 2003.

*Professor, Department of Civil Engineering; chenwq@ccea.zju.edu.cn.
†Associate Professor, Department of Mechanical Engineering.
‡Associate Professor, Department of Civil Engineering.